

# RF-plasma assisted pulsed laser deposition of nitrogen-doped SrTiO<sub>3</sub> thin films

I. Marozau · A. Shkabko · G. Dinescu · M. Döbeli ·  
T. Lippert · D. Logvinovich · M. Mallepell ·  
A. Weidenkaff · A. Wokaun

Received: 12 October 2007 / Accepted: 4 March 2008  
© Springer-Verlag 2008

**Abstract** Perovskite-type nitrogen substituted SrTiO<sub>3</sub> thin films were deposited with a one-step process by RF-plasma assisted pulsed laser deposition from a SrTiO<sub>3</sub> target using a N<sub>2</sub> plasma, while deposition with a NH<sub>3</sub> plasma yields films with almost no incorporated nitrogen. The deposited films exhibit a cubic perovskite-type crystal structure and reveal oriented growth on MgO(100) substrates. The unit cell parameters of the studied N-doped SrTiO<sub>3</sub> films range within  $3.905 < a < 3.918$  Å, which is slightly larger than for SrTiO<sub>3</sub> ( $a = 3.905$  Å). The nitrogen content in the deposited films varies from 0.2 to 0.7 atom%. The amount of incorporated nitrogen in the films decreases with increasing RF-power, while the N<sub>2</sub> flow rate does not have any pronounced influence on the N content. Nitrogen incorporation results in an increased optical absorption at 400–600 nm, which is associated with N(2*p*) energy states that have a higher energy level than the valence band in strontium titanate. The optical band gap energies in the studied N-doped SrTiO<sub>3</sub> films are at 3.2–3.3 eV, which is very similar to that of pure strontium titanate (~3.2 eV). Films deposited with NH<sub>3</sub> for the RF-plasma exhibit a lower degree of crystallinity and reveal almost no nitrogen incorporation into the crystal lattice.

**PACS** 81.15.Fg · 68.55.-a · 81.05.Zx

## 1 Introduction

Miniaturization of Si metal-oxide semiconductor transistors requires an improvement of the dielectric constant and leakage current of the dielectric material. The current choice of materials for gate dielectrics does not fully comply with the need to further reduce the feature size in microchips. Therefore, research has been focused on new materials that exhibit an increase of the dielectric permittivity and a decrease of the leakage current with respect to silicon dioxide [1]. Possible candidates to replace SiO<sub>2</sub> are perovskite-type titanates ATiO<sub>3</sub> ( $A = \text{Sr, Ba}$ ), which reveal relatively high dielectric permittivities and low leakage currents. Substitution of oxygen with nitrogen in these materials can be utilized for a further decrease of the leakage current compared to the pure oxide materials [1, 2]. Thin films can be used as model systems to study the influence of N incorporation and its content on the dielectric properties of these oxynitrides.

Pulsed laser deposition (PLD) of oxides in high vacuum typically results in the formation of oxygen-deficient phases [3] because the light oxygen species (atoms and ions) have a lower sticking probability and a higher scattering degree in the ablation plasma plume, compared to the heavier cationic species. As the oxygen content in the oxides changes their properties dramatically [4], it is very important to control the anionic composition of the deposited material. This point becomes especially important in the case of pulsed laser deposition of films with controlled anionic substitutions. Examples are perovskite-type oxynitrides, which are derived from perovskite-type oxides by partial substitution of O<sup>2-</sup> with N<sup>3-</sup> [5]. There are several approaches to control and/or modify the anionic composition of the growing film. The

---

I. Marozau · T. Lippert (✉) · A. Wokaun  
Paul Scherrer Institut, 5232 Villigen PSI, Switzerland  
e-mail: [thomas.lippert@psi.ch](mailto:thomas.lippert@psi.ch)

A. Shkabko · D. Logvinovich · A. Weidenkaff  
Empa, Überlandstrasse 129, 8600 Dübendorf, Switzerland

G. Dinescu  
National Institute for Lasers, Plasma and Radiation Physics,  
77125 Bucharest-Magurele, Romania

M. Döbeli · M. Mallepell  
Ion Beam Physics, Paul Scherrer Institut and ETH Zurich,  
8093 Zurich, Switzerland

most common technique is to use an appropriate background gas in PLD (e.g.  $O_2$  for deposition of oxides,  $N_2$  or  $NH_3$  for nitrides) [3]. Another possibility is pulsed reactive crossed-beam laser ablation (PRCLA), where a gas pulse is used which is synchronised with the laser and crosses the ablation plume close to its origin [6]. This approach results in an increased reactivity of the gas pulse molecules due to collisions with the highly energetic ablation species in the plasma. In the present work we apply a different technique, which utilises an external source of a continuous plasma beam, generated by RF-discharge [7, 8]. This method has been successfully applied for deposition of different oxide films (with  $O_2$  used for the RF-plasma) and nitride films (with  $N_2$  or  $NH_3$  RF-plasma) [7, 8]. In the paper [8] the authors have shown that utilisation of the reactive RF-induced plasma of nitrogen during pulsed laser deposition of AlN films improves the nitrogen content compared to the films deposited without the nitrogen RF-plasma. In the present study the one-step preparation of N-doped strontium titanate ( $SrTiO_3:N$ ) thin films by RF-plasma assisted PLD using ammonia and nitrogen plasmas, film analysis and characterisation are described.

## 2 Experimental

A scheme of the experimental setup for RF-plasma assisted PLD is presented in Fig. 1. The ionised gas beam (i.e. RF-plasma) is directed to the substrate, which gives additional control over the anionic composition of the films grown by PLD by using different gases for the RF-plasma source. N-doped  $SrTiO_3$  films were deposited by using nitrogen and ammonia RF-plasmas on MgO(100) substrates (1.0 cm by 1.0 cm) with 20 000 pulses. A KrF excimer laser ( $\lambda = 248$  nm) was used at a repetition rate of 10 Hz. The

laser fluence was  $5.0 J cm^{-2}$ , which was found in our previous studies to give a relatively high N content in  $SrTiO_3:N$  films deposited by (PRCLA) [9].

The rod-shaped ceramic  $SrTiO_3$  target was located at a distance of 4.0 cm from the substrate, which was heated to  $650^\circ C$ . The target-to-substrate distance was fixed at 4.0 cm. The nozzle of the RF-plasma source was located at a distance of 6.0 cm from the substrate and the ionised gas beam was directed to the substrate with an angle of  $45^\circ$ . The deposition pressure varied from 37 to 200 Pa depending on the gas used for the RF-plasma and the flow rates (Table 1). A parametric study of the influence of the RF-plasma parameters (RF-power and gas flow rate) on the film proper-

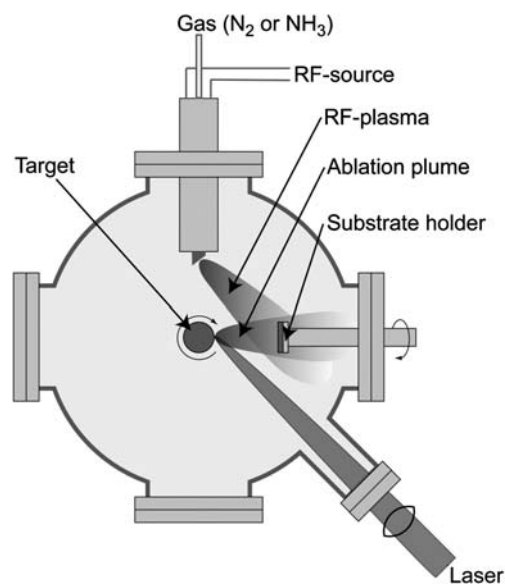


**Fig. 1** Experimental setup for the RF-plasma assisted pulsed laser deposition. A continuous plasma beam (RF-plasma) generated by the RF-discharge is directed to the substrate, which gives additional control over the anionic composition of the film grown by PLD

**Table 1** Properties of N-doped  $SrTiO_3$  thin films deposited by RF-plasma assisted PLD using the  $N_2$  and  $NH_3$  plasmas

Deposition conditions			Deposition pressure, Pa	$a \pm 0.005$ , Å	$d \pm 40$ , nm	$R_q \pm 0.5$ , nm	Nitrogen content, atom%		$E_g \pm 0.1$ , eV
Plasma gas	Gas flow rate, sccm	RF-power, W					[N] $\pm 0.12$ (from XPS)	[N] $\pm 0.3$ (from ERDA)	
$N_2$	50	100	37	3.905	625	18.36	0.67	<0.3	3.29
$N_2$	100	100	67	3.918	365	11.31	0.63	0.66	3.20
$N_2$	150	100	95	3.912	331	10.84	0.68	~0.3	3.20
$N_2$	100	150	66	3.908	391	12.09	0.50	<0.3	3.22
$N_2$	100	200	67	3.910	489	11.69	0.23	<0.3	3.21
$NH_3$	50	100	75	3.912	595	0.78	<0.1		3.23
$NH_3$	100	100	140	3.913	398	3.85	<0.1		3.27
$NH_3$	150	100	200	3.912	345	1.72	<0.1		3.40
$NH_3$	100	150	150	3.912	400	3.69	<0.1		3.18
$NH_3$	100	200	167	3.913	380	4.71	<0.1		3.13

ties was performed. For each gas used in the RF-plasma (i.e. N<sub>2</sub> and NH<sub>3</sub>) two sample series were deposited at different RF-powers and gas flow rates to study the influence of these parameters on the film properties. In the first sample series the gas flow rate of 100 sccm (standard cubic centimetre per minute) was kept constant while the RF-power was varied from 100 to 200 W. In the second sample series the RF-power was fixed at 100 W while the flow rate was varied from 50 to 150 sccm.

The film crystallinity was studied by X-ray diffraction analysis (XRD) using a Siemens D5000 diffractometer in the standard  $\Theta$ - $2\Theta$  mode (CuK $\alpha$  irradiation,  $2\Theta$  range of 20–80°, step 0.005°, 0.3 s/step). To confirm the phase composition grazing incidence X-ray diffraction measurements of some samples were performed on a Phillips X'Pert diffractometer (CuK $\alpha$  irradiation, incident angle of 1°,  $2\Theta$  range of 10–100°, step 0.05°, 0.5 s/step). The film thickness and film roughness were obtained by profilometry (with a Dektak 8 profilometer with a tip size of 5  $\mu\text{m}$ , a load of 3  $\mu\text{g}$ , and a scanning speed of 150  $\mu\text{m s}^{-1}$ ). The chemical composition and the nitrogen content in the films was analysed by elastic recoil detection analysis (ERDA) and X-ray photoelectron spectroscopy (XPS). For the ERDA measurements a 12 MeV <sup>127</sup>I beam was used under 18° incident angle. The scattered recoils were identified by the combination of a time-of-flight spectrometer with a gas ionisation chamber. For the film deposited using the N<sub>2</sub> RF-plasma at a flow rate of 100 sccm and a RF-power of 100 W a detailed depth-profiling ERDA analysis was performed. The XPS spectra were collected at a depth of 50–100 nm after sputtering the film with an Ar<sup>+</sup> ion beam. Transmittance of the films was measured by a Cary 500 Scan UV-Vis-NIR spectrophotometer in the wavelength range of 190–2000 nm (6.5–0.6 eV).

### 3 Results and discussion

#### 3.1 Film deposition

The N<sub>2</sub> and NH<sub>3</sub> RF-plasmas have different optical appearances. The visible part of the nitrogen plasma has a bright orange colour and extends over more than 6 cm from the RF-nozzle, therefore reaching the substrate during the film deposition. The ammonia plasma has a whitish colour, and its visible part of  $\sim 2$ –3 cm is considerably shorter than for nitrogen. The main origin of this different optical appearance of both plasmas is the difference in the lifetime of the emitting excited species. The main emitting species in the ammonia RF-plasma are NH radicals, which exhibit the most intense emission bands in the near-UV region ( $\sim 336$  nm). They decay and recombine relatively fast compared to the excited N<sub>2</sub> molecules—the main emitting species in the nitrogen RF-plasma, which emit in the near UV and visible [10].

Therefore, for the present geometry of the deposition setup, where the nozzle of the RF-plasma source is located at a distance of  $\sim 6$  cm from the substrate, it can be expected that the highly reactive N-containing excited state species in ammonia plasma may decay and recombine before they reach the substrate. This could potentially reduce the amount of nitrogen incorporated into a film using ammonia RF-plasma. However, it is also noteworthy to mention that besides the excited state species that were discussed above, in the RF-induced plasma there might be also non-emitting species containing nitrogen such as ground state radicals and metastables that may have different probabilities to incorporate nitrogen into a growing film.

#### 3.2 Structural characterisation of the films. Film crystallinity and unit cell parameters

In Fig. 2 two typical XRD spectra of the deposited films in comparison with the spectrum of pure MgO(100) substrate are shown. Most of the studied films reveal an oriented growth along the (100) plane direction. However, in addition to the (X00) series of reflections some films reveal also a weak (110) reflection, as indicated for example for the film deposited with N<sub>2</sub> plasma at a RF-power of 150 W and a gas flow rate of 100 sccm (insert in Fig. 2). This additional (110) reflection can be considered as minor compared to the (200), indicating that the studied films reveal a preferential (100) orientation. The intensity of reflections of the films deposited using the NH<sub>3</sub> plasma is much lower than those deposited with N<sub>2</sub> plasma at the same conditions,

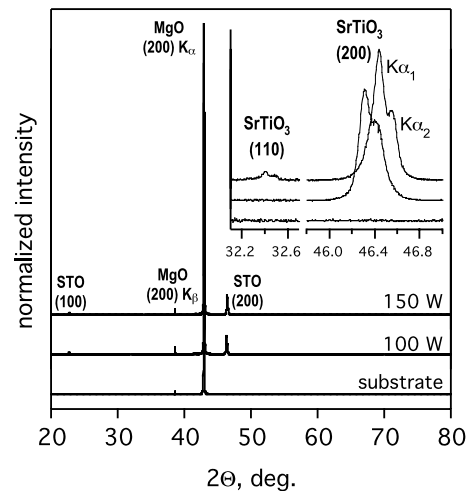


**Fig. 2** Typical XRD patterns of N-doped SrTiO<sub>3</sub> films deposited using a N<sub>2</sub> RF-plasma at a flow rate of 100 sccm. The insert shows the detailed regions around the (110) and (200) film reflections. The observed peak doublets for each crystallographic reflection are due to the K $\alpha_1$  and K $\alpha_2$  lines of the X-ray irradiation source. The film prepared at a RF-power of 100 W reveals an oriented growth along the (100) plane direction. The film deposited at a RF-power of 150 W exhibits in addition a very weak (110) reflection

which indicates a lower degree of crystallinity (i.e. semi-amorphous structure) in the films deposited using the  $\text{NH}_3$  plasma. However, all these films exhibit an oriented growth along the (100) plane direction with no traces of other crystallographic orientations. Studies on the pulsed laser deposition of perovskite-type (La, Ca) $\text{CoO}_3$  films suggest that the presence of the excited state species at the substrate surface during deposition may improve the film crystallinity [11]. Therefore, a shorter RF-plasma beam and a higher deposition pressure for the  $\text{NH}_3$  plasma compared to  $\text{N}_2$  indicates that a considerably smaller amount of the excited species may reach the substrate, which may explain the observed lower degree of crystallinity of the films deposited with the  $\text{NH}_3$  plasma.

The unit cell parameters of the studied films were obtained from the position of the most intense (X00) film reflections. For the films, which exhibit additional minor (110) reflections, no significant differences for the unit cell parameters from the positions of the (X00) reflections or (110) reflections were obtained. This indicates that the crystal structure of the studied films is cubic and that for a film thickness of 330–630 nm no unit cell distortion due to strain effects caused by the lattice mismatch of +7.6% with the  $\text{MgO}(100)$  substrates is detected. The calculated lattice parameters ( $a$ ) of the studied  $\text{SrTiO}_3$ -based films are summarised in Table 1. They are slightly larger compared to that of pure  $\text{SrTiO}_3$  ( $a = 3.905 \text{ \AA}$ ), which can be attributed to the larger crystallographic radius of nitrogen ( $R_{\text{N}} \approx 1.29 \text{ \AA}$ ) compared to oxygen ( $R_{\text{O}} = 1.21 \text{ \AA}$ ) and/or to minor lattice point defects in the films. A typical XRD pattern of a studied strontium titanate based film recorded in the grazing incidence mode is shown in Fig. 3. The PDF card for  $\text{SrTiO}_3$  from the JCPDF database is included as a reference. At the small fixed incident angle of the X-rays of  $1^\circ$  only a very

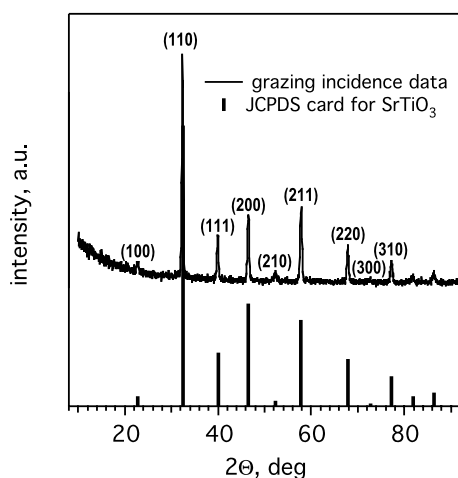


**Fig. 3** Typical grazing incidence diffraction pattern of the N-doped  $\text{SrTiO}_3$  film (deposited using  $\text{N}_2$  RF-plasma at a flow rate of 100 sccm and a RF-power of 100 W). All observed reflections are in agreement with those of  $\text{SrTiO}_3$ , confirming the perovskite-type phase purity

thin rough surface layer of the film is probed by the X-rays. Therefore, the XRD pattern reveals a polycrystalline pattern of the film due to the contribution of the film roughness. The comparison between the diffraction pattern of the film and the PDF card for pure  $\text{SrTiO}_3$  indicates the formation of a single cubic perovskite-type phase with no clear traces of impurities.

### 3.3 Films thickness and roughness

The thickness ( $d$ ) and root-mean-square roughness ( $R_{\text{q}}$ ) of the studied  $\text{SrTiO}_3$ -based films are included in Table 1. In general, two films deposited at the same conditions but with a different gas used for the RF-plasma (i.e.  $\text{N}_2$  and  $\text{NH}_3$ ) reveal a similar thickness despite the relatively large (nearly a factor 2) difference in the deposition pressure (Fig. 4). This indicates that the scattering efficiency of the ablation plasma plume is very different for these two gases, which is most probably due to the different size and mass of the  $\text{N}_2$  and  $\text{NH}_3$  molecules. For a particular gas used in the RF-plasma ( $\text{N}_2$  or  $\text{NH}_3$ ) the films deposited with lower gas flow rates (i.e. at lower deposition pressures) reveal a larger thickness compared to the films deposited at higher flow rates due to the lower scattering at lower deposition pressures. The RF-power has no essential influence on the film thickness deposited at a constant flow rate. The film roughness depends also strongly on the gas used for the RF-plasma. Deposition with  $\text{NH}_3$  plasma results in a relatively low roughness typically in the range of 1–4 nm, whereas deposition with  $\text{N}_2$  plasma yields films with a much higher roughness of about 12–18 nm (Table 1). This difference might be correlated with the lower degree of crystallinity of the films deposited in  $\text{NH}_3$  plasma; i.e. a suppressed construction of the lattice results in a more uniform surface topography. Another possible reason may be the very different main species

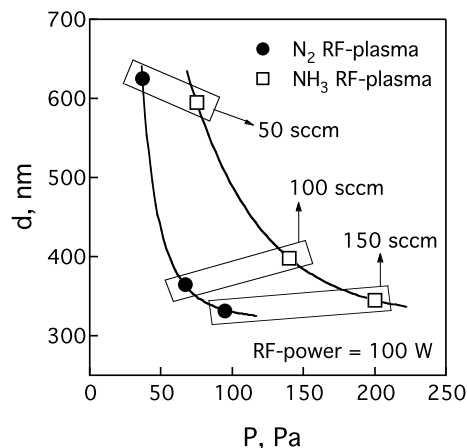


**Fig. 4** Thickness of the  $\text{SrTiO}_3$ -based films deposited by RF-plasma assisted PLD at different flow rates as a function of the deposition pressure. Solid lines are plotted for visual guidance only

in the ammonia and nitrogen RF-plasmas and different propagation length of this species towards the substrate, which might result in different growth mechanisms and therefore film roughness.

### 3.4 N content and chemical composition in the films

Analysis of the nitrogen content in the films was performed by two different techniques: ERDA and XPS. XPS was used as a first method to check the presence of incorporated nitrogen. This technique has a typical probing depth of 2–3 nm in oxide materials, which is considerably smaller than the thickness of the studied films (~350–600 nm). The information obtained by XPS shows therefore only the local composition of the film. The XPS spectra were collected at a depth of 50–100 nm after sputtering with an Ar<sup>+</sup> ion beam to remove the uppermost layer of the film, which may contain absorbed gaseous species from the atmosphere. However, the sputtering can also influence the chemical composition and especially the anionic content in SrTiO<sub>3</sub>-based films due to possible preferential resputtering of oxygen (and, probably, nitrogen) [12]. Therefore, ERDA measurements of the N content were performed on the films with nitrogen as identified by XPS. ERDA is considered to be a non-destructive analytical technique, which allows one to perform composition analysis through the complete film thickness [13]. The disadvantage of ERDA is the lower detection limit of the nitrogen content of ~0.3 atom%, compared to ~0.12 atom% for XPS. The studied films reveal N contents close to the detection limit of ERDA (Table 1). As a result, the nitrogen concentration determined by this technique has a relatively high uncertainty. Therefore, in this particular case XPS is the preferred method to analyse the N content in the films as a function of the RF-plasma parameters. Generally, the results of the nitrogen content measurements by ERDA and XPS are in agreement within the limits of the experimental uncertainties (Table 1, Fig. 6).

Depth-profiling analysis of ERDA data was performed for the film deposited using the N<sub>2</sub> RF-plasma at a flow rate of 100 sccm and a RF-power of 100 W. The atomic concentrations of strontium, titanium and oxygen were analysed as a function of depth in the range of 0–140 nm. The results of this analysis are presented in Fig. 5. No changes in the concentration of these elements were detected within the studied depth range indicating a homogeneous elemental composition of the film.

The nitrogen content ([N]) obtained from ERDA and XPS analysis is included in Table 1. XPS analysis reveals a principal difference between the films deposited with N<sub>2</sub> and NH<sub>3</sub> RF-plasmas; i.e. deposition using N<sub>2</sub> results in N-doped SrTiO<sub>3</sub> films, while deposition with NH<sub>3</sub> yields samples with only traces of incorporated N. As mentioned above, the visible part of the ammonia RF-plasma is considerably smaller for the NH<sub>3</sub> plasma and does not reach the

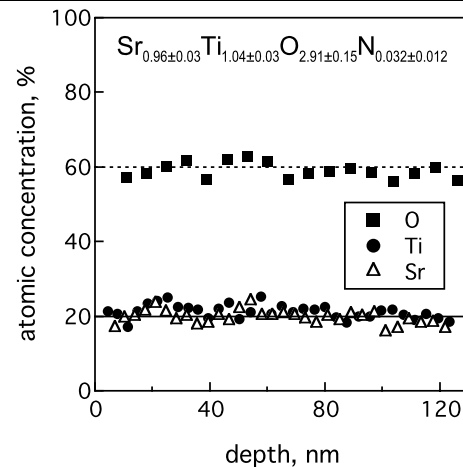
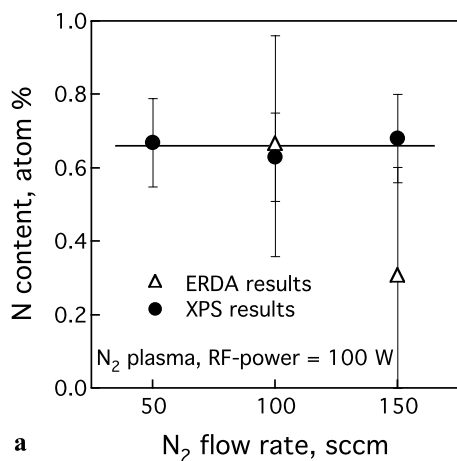


**Fig. 5** ERDA depth-profile of the chemical composition of the film deposited using the N<sub>2</sub> RF-plasma at a flow rate of 100 sccm and a RF-power of 100 W

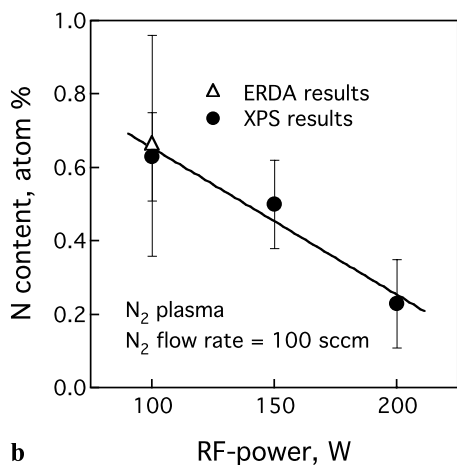
substrate during deposition. The longer plasmas obtained in the case of nitrogen gas is related to the presence of the nitrogen metastables and N atoms in the discharge with relatively long lifetimes. The N<sub>2</sub>(A) state, for example, has a lifetime of ~2 seconds and the N atom recombination is a three body process with a low rate constant at low deposition pressures [10]. These species can therefore easily reach the substrate, which may be beneficial for the nitrogen incorporation into the growing film. The NH radicals in the ammonia RF-plasma have, on the contrary, relatively short lifetimes and decay and recombine before reaching the substrate. As a result, there is almost no nitrogen incorporated into the films grown with the NH<sub>3</sub> plasma at the given distance between the nozzle of the RF-plasma source and the substrate. It is noteworthy that the N content in the films deposited by RF-plasma assisted PLD using the N<sub>2</sub> plasma (~0.2–0.7 atom%) is lower compared to the films deposited by PRCLA under similar conditions using N<sub>2</sub> for the gas pulse (~1.4 atom%) [9]. However, films deposited by PRCLA reveal a relatively high electronic conductivity and cannot be used directly as dielectric or photocatalytically active materials [2, 14], while films deposited by the RF-plasma assisted PLD are insulators.

Figure 6 presents the nitrogen content in N-doped SrTiO<sub>3</sub> films as a function of the N<sub>2</sub> flow rate and RF-power applied to create the plasma. XPS analysis reveals no significant variations of the N content at flow rates of 50–150 sccm (Fig. 6a), while ERDA shows no clear trend, probably due to the nitrogen content in the studied films being close to the detection limit of this technique. Increasing the N<sub>2</sub> flow rate results in a higher amount of excited nitrogen species (molecules, ions and atoms), which reach the substrate during the film growth. However, a higher flow rate through the RF-discharge cavity results in a lower plasma excitation degree, and therefore a lower amount of reactive nitrogen species

in the plasma beam. The total deposition pressure increases also with increasing flow rates, which causes a higher degree of interaction of the  $N_2$  plasma with the background gas. This lowers also the reactivity of the nitrogen species in the RF-plasma beam due to collisions with the background gas. The amount of incorporated N remains almost constant as a result of these two counteracting effects within the studied range of the nitrogen flow rates (Fig. 6a). The N content in the films deposited using the  $N_2$  RF-plasma decreases gradually with an increase of the RF-power in the range of 100–200 W (Fig. 6b). The plasma ionisation degree increases generally with increasing applied RF-power for a fixed nitrogen flow rate. Therefore, the observed decrease of the N content in the films suggests that with increasing RF-power nitrogen species with lower reactivity are formed, which are not incorporated into the crystal lattice of the growing film. One possible explanation is that ions, which are increasingly formed in the plasma beam with increasing RF-power, have



a



b

**Fig. 6** Nitrogen content in N-doped  $SrTiO_3$  films deposited using  $N_2$  RF-plasma as a function of (a) nitrogen flow rate; (b) RF-power applied to create the plasma. Solid lines are plotted for visual guidance only. For the films deposited at a  $N_2$  flow rate of 50 sccm (a) and RF-powers of 150 and 200 W (b) ERDA analysis suggests a N content <0.3 atom%

a lower probability to be incorporated into the growing film compared to excited neutral species and metastables. Further experiments have to be performed in order to study the behaviour and influence of different excited species in  $NH_3$  and  $N_2$  RF-plasmas on the formation of oxynitride phases in RF-plasma assisted PLD as a function of the RF-power.

### 3.5 Optical properties of the films

Figure 7 shows the typical transmittance spectra of the  $SrTiO_3$ -based films deposited with  $N_2$  and  $NH_3$  RF-plasmas. The spectra reveal a broad absorption band at wavelengths below  $\sim 380$  nm. The optical band gap energies ( $E_g$ ) can be determined from the position of the absorption edge. The results of these calculations are shown in Table 1. The optical band gap energies in the studied strontium titanate-based films are close to that of pure  $SrTiO_3$  ( $\sim 3.2$  eV). The transmittance spectra of the N-doped films (deposited using  $N_2$  plasma) contain also an additional absorption shoulder in the visible region around 400–600 nm. On the basis of electronic structure calculations [14] this absorption shoulder may be related to isolated  $N(2p)$  orbitals, which form isolated energy levels inside the forbidden energy band gap above the valence band formed by the  $O(2p)$  orbitals. The presence of these  $N(2p)$  levels enables electron excitations from them to the conduction band with energies lower than the band gap energy. This means that photons in the visible can be absorbed, suggesting a potential application of N-doped perovskites as photocatalysts using visible light. The transmittance spectra of the films with minor N content (deposited in  $NH_3$  RF-plasma) reveal no absorption shoulder at 400–600 nm; i.e. they remain transparent in the visible (Fig. 7). This confirms that the absorption at 400–600 nm is

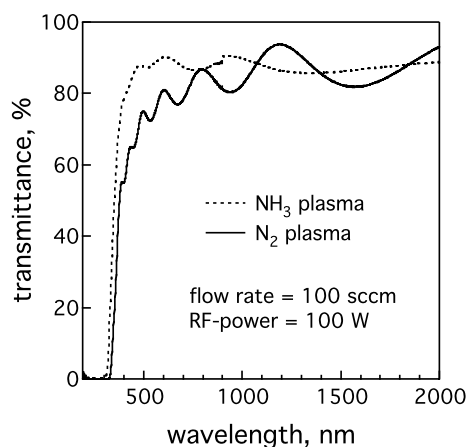


**Fig. 7** Typical transmittance spectra of the studied  $SrTiO_3$ -based films. N-doped films deposited in  $N_2$  RF-plasma reveal an absorption shoulder in the visible range of wavelength ( $\sim 400$ – $600$  nm), which is associated with nitrogen incorporation into the perovskite-type crystal lattice. The oscillations above 500 nm are due to interference phenomena

due to the N incorporation into the crystal lattice of strontium titanate, assuming that the lower crystallinity of the films deposited with the NH<sub>3</sub> RF-plasma is not related to the observed difference of absorption in the visible.

#### 4 Conclusions

The applicability of RF-plasma assisted PLD for the deposition of perovskite-type oxynitrides has been tested and the influence of the RF-plasma parameters on the film properties was studied. Preferentially (100)-oriented N-doped strontium titanate films were deposited on MgO(100) substrates using a N<sub>2</sub> RF-plasma, while deposition with an NH<sub>3</sub> plasma results in films with a lower degree of crystallinity and a very low amount of incorporated nitrogen. The N concentration in SrTiO<sub>3</sub>:N films deposited using the N<sub>2</sub> RF-plasma varies from 0.2 to 0.7 atom%. The films are insulators (the in-plane resistance is higher than 40 MΩ) and reveal no electronic conductivity as previously observed in anion deficient N-doped SrTiO<sub>3</sub> films deposited by PRCLA. This allows to analyze SrTiO<sub>3</sub>:N films prepared by RF-plasma assisted PLD as potential dielectric materials. N incorporation results also in an increased absorption of the visible light, which suggest a possible application as photocatalytically active materials.

**Acknowledgement** This work is partially supported by MaNEP, Paul Scherrer Institut, Empa, and the Romanian RD CEEX program.

#### References

1. D.S. Wu, R.H. Horng, F.C. Liao, C.C. Lin, *J. Non-Cryst. Solids* **280**, 211 (2001)
2. N. Kohara, A. Yoshida, T. Sawada, M. Kitagawa, *Jpn. J. Appl. Phys. Part 1 Regul. Pap. Short Notes Rev. Pap.* **39**, 3519 (2000)
3. R. Perez-Casero, J. Perriere, A. Gutierrez-Llorente, D. Defourneau, E. Millon, W. Seiler, L. Soriano, *Phys. Rev. B Condens. Matter* **75**, 165317 (2007)
4. H.P.R. Frederikse, W.R. Thurber, W.R. Hosler, *Phys. Rev.* **134**, A442 (1964)
5. F. Tessier, R. Marchand, *J. Solid State Chem.* **171**, 143 (2003)
6. P.R. Willmott, R. Timm, J.R. Huber, *J. Appl. Phys.* **82**, 2082 (1997)
7. S. Canulescu, G. Dinescu, G. Epurescu, D.G. Matei, C. Grigoriu, F. Craciun, P. Verardi, M. Dinescu, *Mater. Sci. Eng. B* **109**, 160 (2004)
8. A. Basillais, R. Benzerga, H. Sanchez, E. Le Menn, C. Boulmer-Leborgne, J. Perriere, *Appl. Phys. A* **80**, 851 (2005)
9. I. Marozau, M. Döbeli, T. Lippert, D. Logvinovich, M. Mallepell, A. Shkabko, A. Weidenkaff, A. Wokaun, *Appl. Phys. A Mater. Sci. Process.* **89**, 933 (2007)
10. R.W.B. Pearse, A.G. Gaydon, *The Identification of Molecular Spectra* (Chapman and Hall, London, 1976)
11. M.J. Montenegro, T. Lippert, A. Weidenkaff, A. Wokaun, in *Nanophotonics: Integrating Photochemistry, Optics, and Nano/Bio-Materials Studies*, ed. by H. Masuhara, S. Kawata (Elsevier, Amsterdam, 2004), p. 251
12. K.J. Kim, D.W. Moon, S.H. Nam, W.J. Lee, H.G. Kim, *Surf. Interface Anal.* **23**, 851 (1995)
13. W.K. Chu, J.W. Mayer, M.A. Nicolet, *Backscattering Spectrometry* (Academic Press, San Diego, 1978)
14. M. Miyauchi, M. Takashio, H. Tobimatsu, *Langmuir* **20**, 232 (2004)